Journal of ELECTRONIC MATERIALS, Vol. 47, No. 9, 2018
https://doi.org/10.1007/s11664-018-6300-z

TOPICAL COLLECTION: 17TH CONFERENCE ON DEFECTS (DRIP XVII)

W and X Photoluminescence Centers in Crystalline Si: Chasing Candidates at Atomic Level Through Multiscale Simulations

MARÍA ABOY,[1,2] IVÁN SANTOS,[1] PEDRO LÓPEZ,[1] LUIS A. MARQUÉS,[1] and LOURDES PELAZ[1]

1.—Dpto. Electricidad y Electrónica, E.T.S.I. Telecomunicación, Universidad de Valladolid, Paseo Belén 15, 47011 Valladolid, Spain. 2.—e-mail: marabo@tel.uva.es

Several atomistic techniques have been combined to identify the structure of defects responsible for X and W photoluminescence lines in crystalline Si. We used kinetic Monte Carlo simulations to reproduce irradiation and annealing conditions used in photoluminescence experiments. We found that W and X radiative centers are related to small Si self-interstitial clusters but coexist with larger Si self-interstitials clusters that can act as nonradiative centers. We used molecular dynamics simulations to explore the many different configurations of small Si self-interstitial clusters, and selected those having symmetry compatible with W and X photoluminescence centers. Using *ab initio* simulations, we calculated their formation energy, donor levels, and energy of local vibrational modes. On the basis of photoluminescence experiments and our multiscale theoretical calculations, we discuss the possible atomic configurations responsible for W and X photoluminescence centers in Si. Our simulations also reveal that the intensity of photoluminescence lines is the result of competition between radiative centers and nonradiative competitors, which can explain the experimental quenching of W and X lines even in the presence of the photoluminescence centers.

Key words: Photoluminescence, crystalline silicon, irradiation defect clusters, multiscale atomistic simulations

INTRODUCTION

Photoluminescence (PL) spectra of crystalline Si (*c*-Si) show peaks with energies below the energy bandgap associated with PL centers formed by defects involving dopants or impurities.[1–3] However, the origin of certain peaks remains unclear. Elucidating the nature of unknown PL centers can improve the capabilities of the PL technique to identify lattice defects. Also, the possibility of converting Si into a subbandgap light-emitting semiconductor based on introduction of PL centers has been explored.[4,5] Among such PL lines with unclear origin, W (1018 meV) and less intense X (1040 meV) lines are observed after implantation at low dose, and their intensity can be maximized after subsequent thermal annealing or irradiation at elevated temperature (250°C to 500°C).[6,7]

Identification of the associated PL centers directly from experiments is difficult, as irradiation generates a large variety of defects that coexist with these radiative defects. The intensity of a particular PL line depends on the capture of photogenerated carriers by PL centers in competition with other radiative or nonradiative defects in their vicinity. Based on the results of positron annihilation and photoluminescence experiments in ion-implanted crystalline Si, Harding et al. proposed small vacancy clusters as possible nonradiative recombination centers responsible for the quenching of the W line observed as the Si implantation dose was increased.[6,8,9] In addition, in boron-implanted crystalline Si samples, the interaction among dopant atoms and defects influenced the PL intensity of W and X lines.[10] This had been attributed to formation

(Received November 16, 2017; accepted April 11, 2018; published online April 25, 2018)

of additional radiative[11] or nonradiative recombination centers[12] that compete in the capture of photogenerated carriers with PL centers that exist in undoped samples. Despite this complex scenario, some features of the defects responsible for W and X lines are known from experiments, namely that they consist of Si self-interstitial clusters (I_n)[6,7] and that the W center has trigonal symmetry while the X center has tetragonal symmetry,[1–3] and their high-energy local vibrational modes (LVMs) have been measured.[1–3,13] In the work presented herein, we used a multiscale simulation approach to explore the possible structure of defects responsible for W and X lines by comparison of this experimental evidence with the results of appropriate simulation techniques.

KINETIC MONTE CARLO SIMULATIONS

We used nonlattice kinetic Monte Carlo (KMC) simulations to reproduce irradiation and annealing conditions used in PL experiments and to extract the relevant I_n size distribution. Simulation of implantation cascades was performed within the binary collision approximation, which provides the coordinates of Si self-interstitials, vacancies, and implanted ions. This information was transferred to the KMC code to simulate annealing at the implantation temperature.[14] Interactions among defects and dopants must be specified, and their energetics (migration barriers, binding energies, etc.) defined. In our simulations, we used migration and formation energies for Si self-interstitials and vacancies reported in Ref. 14.

The changes in the PL intensity of the W line under different irradiation conditions were studied experimentally by Giri et al.[9] They considered *c*-Si samples implanted with 80-keV Si ions at 265°C, conditions that are known to maximize the PL intensity of the W line.[6,7] To provide understanding on the distribution of the W center, they varied the implantation dose in the range of 10^{13} cm^{-2} to 3×10^{14} cm^{-2}, and afterwards removed the implanted surface up to depth of 200 nm and 255 nm. Figure 1a plots the PL intensity of the W line as a function of the implantation dose for the as-implanted sample, as well as for the samples etched to depth of 200 nm and 255 nm. The results of those experiments showed that the W-line intensity decreased with implantation dose for the as-implanted sample. In contrast, after surface removal, the PL intensity initially increased with implantation dose then saturated. Moreover, after removal of the top surface, the PL intensity was lower than in the as-implanted sample for low implantation doses, but for high implantation doses it became higher than in the as-implanted sample.

We performed KMC simulations with the implantation conditions of Giri's experiments, monitoring the amount and distribution of I_n clusters for each size n. Figure 1b plots the simulated density of I_n clusters of different sizes as a function of implantation dose, while Fig. 1c and d shows the simulated I_n depth distribution for implantation dose of 10^{13} cm^{-2} and 10^{14} cm^{-2}, respectively. The results of these KMC simulations indicate that the density of all I_n increases with implantation dose (Fig.1b). However, it is noteworthy that the increment is more significant for larger clusters ($n > 6$) than for smaller ones ($n \leq 5$). In principle, the experimentally observed decrease in the W-line PL intensity with implantation dose in the as-implanted sample (Fig. 1a) should be associated with a decrease in the density of the I_n responsible for W PL with increasing implantation dose. These simulation results suggest that the W line could be due to small I_n, whereas larger clusters could act as nonradiative competitors. This hypothesis is compatible with the experimental changes in the PL intensity for the sample etched to depth of 255 nm compared with the as-implanted sample (Fig. 1a). The results of these simulations show that small I_n ($n \leq 5$) are dominant in the etched region for low implantation dose (Fig. 1c). Therefore, the reduction of the W-line PL intensity observed experimentally for 10^{13} cm^{-2} could be due to removal of a high concentration of the small I_n that could be responsible for the W line. In contrast, simulations show that, for the higher implantation dose (Fig. 1d), large I_n ($n > 6$) are dominant in the 255-nm etched region. Therefore, the increase in the W-line PL intensity reported for the samples etched to 255 nm at high implantation

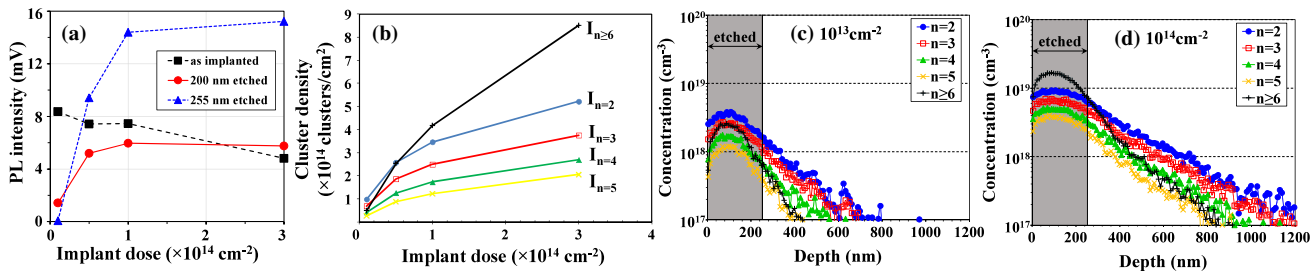

Fig. 1. (a) W-line PL intensity as function of implantation dose and etching depth (data taken from Ref. 9). (b) Density of I_n for different cluster sizes, n, after implantation with 80-keV Si ions at 265°C at several doses from KMC simulations. (c, d) Depth concentration profiles of I_n at those implantation conditions. Shaded areas represent the 255-nm etched layer of Ref. 9.

doses could be due to removal of a high percentage of the large I_n that act as nonradiative competitors. Equivalent results were obtained from experiments studying the X PL line (not shown).

Previous works by Harding et al.[6,8] proposed small vacancy clusters as the quenching mechanism for the W line. These authors analyzed the Si-ion implantation conditions required to quench the PL intensity of the W line in crystalline Si, using 4-MeV implantation energy in their experiments. A combination of PL measurements with the variable-energy positron annihilation spectroscopy technique (which is only sensitive to vacancy defects) was used, revealing a correlation between the quenching of the W line and the concentration of small vacancy clusters in the vacancy-rich region typically obtained near the surface after implantation at $\sim$ MeV.[15] We do not deny that small vacancy clusters act as nonradiative centers and are thus responsible for the quenching of the PL intensity of the W line reported under the particular experimental conditions analyzed in that article. In the case of $\sim$ keV implantation, as was the case for the experiments considered in the present work,[9] the different spatial separation among Si interstitial and vacancy distributions is less significant in the surface region. Our simulations show that the vacancy profile almost overlaps with that for Si interstitials (not shown). We observed that the evolution of all vacancy clusters increased with implantation dose throughout the whole damage profile for all implantation doses, with V_2 and V_3 clusters being dominant. In contrast, for Si interstitial clusters (Fig. 1b), the density of small Si interstitial clusters is dominant for low implantation doses whereas the density of large Si interstitial clusters becomes comparable or even exceeds the density of smaller ones as the implantation dose is increased. In addition, the depth profiles show that these large clusters (whose density increases significantly with implantation dose) are dominant in the surface region (0 nm to 250 nm) (Fig. 1c and d). Therefore, the results of these simulations suggest that the most significant difference between low and high implantation dose as well as between unetched and etched samples lies in the presence of large Si interstitial clusters. For all these reasons, we propose large Si interstitial clusters as candidate nonradiative centers responsible for the quenching of the W line in the particular experiments reported by Giri et al.[9]

CLASSICAL MOLECULAR DYNAMICS SIMULATIONS

On the basis of our KMC simulations, we assumed that W and X centers consist of small I_n ($n \leq 5$). However, the particular cluster size and structure of defects responsible for these PL lines cannot be inferred from KMC simulations. Therefore, we used classical molecular dynamics (CMD) simulations to explore the many different atomic configurations of small I_n ($n \leq 5$). In particular, we used the code LAMMPS,[16] describing Si–Si interactions using the Tersoff 3 empirical potential.[17] We introduced a number n of Si self-interstitials at neighboring positions in the simulation cells. We carried out annealing simulations at 1200 K during 25 ns, so the introduced defects form a I_n and its atomic configuration could evolve.

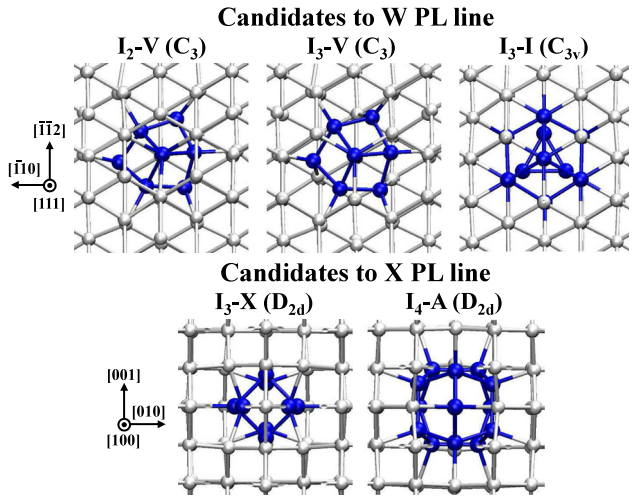

Fig. 2. Defect candidates for W (upper row) and X (lower row) PL centers. Atomic projections on convenient planes are shown to highlight their symmetry, which is indicated in parenthesis. Si lattice atoms and Si atoms of the defect are represented by white and blue spheres, respectively. Differences between I_2-V and I_3-V configurations are not evident in the selected projection. For more details see Ref. 26.

We found more than 100 configurations for I_n ($n \leq 5$) from atom dynamics, without assuming any preestablished defect configuration. Among these, we selected those with the trigonal symmetry of the W center,[2] and the tetragonal symmetry of the X center.[3] Selected configurations are shown in Fig. 2. For the W center, we found a di-interstitial defect and a tri-interstitial cluster configuration previously reported by Carvalho et al., known as I_3-V.[18] The di-interstitial defect is labeled as I_2-V, since it is very similar to the I_3-V defect configuration. It is noteworthy that the presented I_3-I tri-interstitial cluster was not obtained from our CMD simulations. As it was previously assigned to the W center by Carvalho et al.,[18] we considered it in our analysis for completeness. For the X center, we found a tri-interstitial defect previously reported by Bondi et al.[19], denoted hereinafter as I_3-X, and the tetra-interstitial cluster configuration proposed by Arai et al.[20] and considered as the X center by Carvalho et al.,[18] denoted hereinafter as I_4-A.

Ab Initio SIMULATIONS

To determine whether our selected defects are compatible with radiative transitions of W and X

centers, an electronic description of the system is required, which cannot be afforded by the simulation techniques presented above. We resorted to *ab initio* simulations to determine whether the I_n selected from CMD simulations are compatible with radiative transitions of W and X centers. We used the VASP code[21,22] with Perdew–Burke–Ernzerhof (PBE)–projector augmented wave (PAW) pseudopotentials[23,24] to characterize (1) the electronic band structure of defects, which shows whether a defect might favor or not radiative recombinations; (2) the defect formation energy, in order to obtain the defect levels within the energy bandgap to relate them with experimental PL photon energies[25]; and (3) the LVMs, which can be directly compared with the experimental values observed in PL spectra.[26]

Since PL lines are associated with radiative recombinations, the electronic band structure of defects responsible for W and X PL lines should favor direct transitions. Figure 3 shows the calculated electronic band structure of I_2-V and I_3-V defects, two of the candidates for the W center, along with the band structure of *c*-Si for comparison. The band structure of I_2-V shows two bands within the energy bandgap, leading to its rejection as a radiative center. For this reason, we do not consider the I_2-V defect in the discussion below. In contrast, the band structure of I_3-V shows a new band at the top of the valence band, and the bottom of the conduction band is modified. These modifications in the electronic band structure with respect to *c*-Si suggest that direct transitions between band edges might be possible, and so might be radiative recombinations. The electronic band structures of I_3-I, I_3-X, and I_4-A (not shown) are also compatible with radiative recombinations.

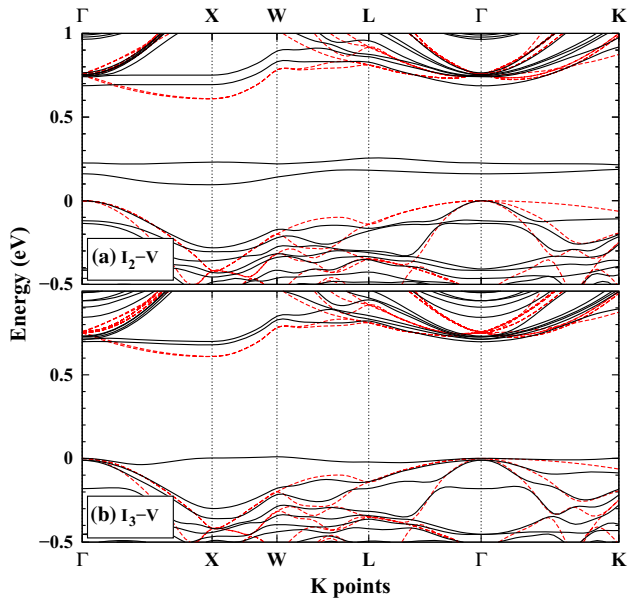

Fig. 3. Band structure modifications induced by (a) I_2-V and (b) I_3-V defects in their neutral charge state. The band structure of *c*-Si is also shown by red dashed lines for comparison.

Table I summarizes other quantities calculated from *ab initio* simulations for the defects in Fig. 2 with band structure compatible with radiative transitions. For each defect, we report: (1) its formation energy for neutral charge state, $E_f[D^0]$; (2) its donor level of defects, $E_{0/+}$, with respect to the valence band edge; and (3) the energies of their LVMs, E_{Ph}. Details of these calculations can be found in Ref. 26. It is noteworthy that I_3-I, considered by Carvalho et al. as the W center, has the highest energy of formation among the I_3 defects considered in our study, thus being the most unstable. In fact, I_3-I was not obtained from our CMD simulations, nor in long-time tight-binding molecular dynamics simulations.[27]

Regarding the energy levels introduced within the energy bandgap, we found that defects considered in Table I only have a $E_{0/+}$ donor level, but no $E_{0/-}$ acceptor level. We estimated the expected donor level of W and X PL centers from the energy difference between the *c*-Si bandgap and the experimental photon energies (E_{PL}), as indicated in Eq. 1. The exciton binding energy is neglected in Eq. 1, as it is about one-tenth of the carrier binding energy to the defect.[28]

$$E_{0/+}^{\text{expected}} \simeq E_g(c\text{–}Si,\ Low\ \mathrm{T}) - E_{PL}. \quad (1)$$

Table I. Properties of I_3-V, I_3-I, I_3-X, and I_4-A from Fig. 2 obtained from *ab initio* simulations: formation energy for neutral configurations ($E_f[D^0]$), calculated and expected donor levels of defects ($E_{0/+}$) (see text for details), and high-energy LVMs at the point (E_{Ph})

Line	Defect	$E_f[D^0]$ (eV)	$E_{0/+}$ (eV)		E_{Ph} (meV)	
			This work	Expected	This work	Experiments
W	I_3-V	6.74	0.13	∼ 0.15	68.2, (59.9, 59.9)	70, 60, 56, 51 (Ref. 2)
	I_3-I	7.50	0.08		74.8, 74.8, 74.5, 70.8	
X	I_3-X	6.99	0.14	∼ 0.13	62.8, 62.6, (61.6, 61.5)	69.0, 67.9, 66.2 (Ref. 13)
	I_4-A	7.42	0.19		63.6, (63.2, 63.2), 62.4	

Parentheses in E_{Ph} energies group LVMs with equivalent atomic movements.

Thus, the expected donor levels of W and X PL centers should be $\sim$ 0.15 eV and $\sim$ 0.13 eV, respectively, with respect to the valence band edge, considering an energy gap for *c*-Si close to 1.17 eV (as PL experiments are commonly performed at very low temperatures $\sim$ 4 K to 20 K). Results shown in Table I indicate that I_3-V is in better agreement with the donor level of the W center than I_3-I, while for the X center the better agreement is for I_3-X.

Finally, the LVMs of selected defects can be directly compared with the peaks that appear in the phonon side-bands of zero-phonon lines in PL spectra. Taking into account that generalized gradient approximation (GGA) pseudopotentials tend to lower the energies of the LVMs,[29] the better agreement among the defect candidates for the W center is for I_3-V, while for the X center both I_3-X and I_4-A show very similar values, lying slightly below experimental results.

CONCLUSIONS

We used a multiscale simulation approach to identify and characterize I_n configurations as candidate W and X photoluminescence centers in *c*-Si. We found that the so-called I_3-V is the most likely candidate for the W PL center. For the X center, the so-called I_3-X defect seems the most likely candidate, but we cannot determine this conclusively, as not all its properties fit the experimental features within the accuracy of our calculations. Nevertheless, note that the evolution of the W and X PL results not only from the evolution of the defects responsible for them. Other coexisting defects could act as nonradiative competitors that could quench the luminescence from the W and X photoluminescence centers in *c*-Si. Therefore, optimization of the PL intensity involves not only maximization of radiative defect formation but also removal of nonradiative defects.

ACKNOWLEDGEMENTS

This work has been supported by the EU (FEDER) and the Spanish Ministerio de Ciencia e Innovación under Project No. TEC2014-60694-P, and by the Junta de Castilla y León under Project No. VA331U14. The authors thank the Spanish Supercomputing Network for computational time provided through Project No. QCM-2014-3-0034.

REFERENCES

1. G. Davies, *Phys. Rep.* 176, 83 (1989).
2. G. Davies, E.C. Lightowlers, and Z.E. Ciechanowska, *J. Phys. C: Solid State Phys.* 20, 191 (1987).
3. Z.E. Ciechanowska, G. Davies, and E.C. Lightowlers, *Solid State Commun.* 49, 427 (1984).
4. J. Bao, M. Tabbal, T. Kim, S. Charnvanichborikarn, J.S. Williams, M.J. Aziz, and F. Capasso, *Opt. Express* 15, 6727 (2007).
5. S. Buckley, J. Chiles, A.N. McCaughan, G. Moody, K.L. Silverman, M.J. Stevens, R.P. Mirin, and S.W. Nam, J.M. Shainline, *Appl. Phys. Lett.* 111, 141101 (2017).
6. R.E. Harding, G. Davies, P.G. Coleman, and C.P. Burrows, *J. Wong-Leung, Phys.* B 738, 340 (2003).
7. B.C. Johnson, B.J. Villis, J.E. Burgess, N. Stavrias, J.C. McCallum, S. Charnvanichborikarn, J. Wong-Leung, C. Jagadish, and J.S. Williams, *J. Appl. Phys.* 111, 094910 (2012).
8. R.E. Harding, G. Davies, S. Hayama, P.G. Coleman, and C.P. Burrows, *J. Wong-Leung, Appl. Phys. Lett.* 89, 181917 (2006).
9. P.K. Giri, S. Coffa, and E. Rimini, *Appl. Phys. Lett.* 78, 291 (2001).
10. S. Charnvanichborikarn, B. Villis, B. Johnson, J. Wong-Leung, J. McCallum, J. Williams, and C. Jagadish, *Appl. Phys. Lett.* 96, 051906 (2010).
11. J. Adey, J.P. Goss, R. Jones, and P.R. Briddon, *Phys. Rev.* B 67, 245325 (2003).
12. M. Aboy, I. Santos, L. Pelaz, L. Marqués, and P. López, *2011 IEEE Spanish Conference on Electron Devices*, p. 051906 (2011).
13. S. Hayama, G. Davies, and K.M. Itoh, *J. Appl. Phys.* 96, 1754 (2004).
14. L. Pelaz, L.A. Marqués, M. Aboy, P.López, and I. Santos, *Eur. Phys. J.* B 72, 323 (2009).
15. S. Chakravarthi and S. Dunham, *J. Appl. Phys.* 89, 4758 (2001).
16. S. Plimpton, *J. Comp. Phys.* 117, 1 (1995). http://lammps.sandia.gov.
17. J. Tersoff, *Phys. Rev. B* 38, 9902 (1988).
18. A. Carvalho, R. Jones, J. Coutinho, and P.R. Briddon, *Phys. Rev. B* 72, 155208 (2005).
19. R. Bondi, S. Lee, and G. Hwang, *Phys. Rev. B* 80, 125202 (2009).
20. N. Arai, S. Takeda, and M. Kohyama, *Phys. Rev. Lett.* 78, 4265 (1997).
21. G. Kresse and J. Furthmuller, *Comput. Mater. Sci.* 6, 15 (1996).
22. G. Kresse and J. Furthmuller, *Phys. Rev. B* 54, 11169 (1996).
23. J.P. Perdew, K. Burke, and M. Ernzerhof, *Phys. Rev. Lett.* 77, 3865 (1996).
24. G. Kresse and D. Joubert, *Phys. Rev. B* 59, 1758 (1999).
25. C. Freysoldt, B. Grabowski, T. Hickel, J. Neugebauer, G. Kresse, A. Janotti, and C.V. de Walle, *Rev. Mod. Phys.* 86, 253 (2014).
26. I. Santos, M. Aboy, P. López, L.A. Marqués, and L. Pelaz, *J. Phys. D: Appl. Phys.* 49, 075109 (2016).
27. D.A. Richie, J. Kim, S.A. Barr, K.R.A. Hazzard, R. Hennig, and J.W. Wilkins, *Phys. Rev. Lett.* 92, 045501 (2004).
28. I. Pelant, J. Valenta, *Experimental Techniques of Luminescence Spectroscopy* (Oxford University Press, 2012), chap. 7, p. 186.
29. F. Favot and A. Dal Corso, *Phys. Rev. B* 60, 11427 (1999).